Spin resonance canceling lattice cell design principles

V. H. Ranjbar
Brookhaven National Laboratory, Upton, New York 11973, USA

(Received 9 January 2023; accepted 22 May 2023; published 5 June 2023)

We show how to construct an accelerator lattice cell that minimizes all intrinsic spin resonances. We then apply this approach to various toy electron and proton accelerators, considering, AGS-booster, AGS-like and CEPC/FCC-ee, and FCC-hh-like rings.

DOI: 10.1103/PhysRevAccelBeams.26.061001

I. INTRODUCTION

The development of accelerators that can maintain high polarization for particle beams remains important for both nuclear and high energy physics experiments. Polarization is critical both for energy calibration and the actual interactions being probed. The use of magnets known as Siberian snakes [1] has opened up the high energy sector to polarized hadron beams, however, it has its limitations. Siberian snakes work by rotating the polarization at regular azimuthal locations in the ring in such a way as to cancel the low order spin kicks developed in a given lattice. For protons, a helical design uses radial fields which permit spin rotations that are relatively transparent optically and require field strengths that are very weakly dependent of energy. However, for electrons, the radial fields at low energies lead to orbit excursions beyond the beam's physical aperture, and at higher energies, these same fields can cause excessive synchrotron radiative losses. As such solenoids are usually used for electrons [2], yet these can have a significant impact on the optics and spin diffusion as well they are difficult to ramp to match an accelerating lattice and the peak fields for high energy electrons can become technically very challenging. For hadrons, as the energy goes higher, the net strength of the perturbing spin kicks grows larger and more snakes are required. As well often there might not be enough space for functioning full snake in a given lattice [as in the case of Brookhaven National Laboratory's (BNL) alternating gradient synchrotron (AGS)].

As such, the development of lattice design approaches that can minimize the strength of spin resonances is desirable. The optics design for suppressing intrinsic resonances is often referred to as "spin matching." In different variants, it has been applied in proton rings, as the alternating gradient synchrotron (AGS) [3] and the cooler synchrotron (COSY) [4], as well as in the $e^{\pm}$ ring of the Hadron Elektron Ring Anlage (HERA) [5] for minimizing the intrinsic resonances introduced by spin rotators.

However, these approaches usually only work for a particular energy and to address spin resonances at other energies, a "continuous" optics change is needed. This process, if possible, may be very impractical. In addition to this, there have been proposals to build lattices where the individual quadrupoles are split into two with a dipole inserted between them. The vertical field from the dipole would then rotate the spin by 180°, in this way minimizing the spin kick from the quadrupole [6]. In this paper, we present a new lattice design approach to suppress spin resonances for all energies.

II. SPIN KICKS IN THE ARC CELLS

The transport of spin polarized beam across a standard arc focusing and defocusing lattice (FODO) may introduce transverse spin kicks that can accumulate between dipoles. These spin kicks will, for an appropriate spin tune, add up coherently and lead to beam depolarization marked by the presence of an intrinsic spin resonance. However, if the quadrupole's location and strength can be organized correctly, the transverse spin kicks can cancel or be minimized for all spin tunes. This is somewhat similar to what is known as spin matching at a particular spin tune. However, since the cancelation occurs between spin precessing dipoles, this makes the spin matching condition work for all energies and spin tunes. The development of the design for the future Electron-Ion Collider's (EIC's) rapid cycling synchrotron (RCS) required arc connecting regions that would not contribute to the intrinsic spin resonances [7]. This was initially accomplished by ensuring that the betatron phase advance was an integer multiple of 2π, in the straight arc connecting lattice. In this paper, we consider the case when it is not possible to achieve a full 2π phase advance in a given straight, in particular, arc cell where the drift distance between dipoles is too short.

III. SPIN PROPERTIES OF FODO CELL

A standard FODO cell contains focusing and defocusing quadrupoles with a dipole placed between them. In this situation, there is no possibility of cancelation of the spin kick between dipoles. Another type of FODO cell includes the dipoles on either end of the focusing and defocusing string of quadrupoles.

We can estimate the contributions to intrinsic spin resonances by considering the terms of the vertical betatron spin resonance integral [8]

$$\mathrm{w}_{\kappa_0} = \lim_{N_T\to\infty}\frac{-1}{2\pi N_T}\int_0^{LN_T}\left[(1+a\gamma)\left(y''+\frac{iy'}{\rho}\right) - i(1+a)\left(\frac{y}{\rho}\right)'\right]e^{i\kappa_0\theta(s)}\mathrm{d}s. \quad (1)$$

Here L is the lattice length and N_T the number of turns. This equation makes use of the standard Frenet-Serret coordinate system for y and s (see Fig. 1) and θ is the accumulated bending angle with κ_0 the spin resonance tune and a the gyromagnetic anomaly, ρ being the design horizontal bending radius which is large with respect to the orbital coordinates. In this equation, y can represent vertical motion both due to betatron motion and due to orbit imperfections. It assumes that the spin closed orbit ($\hat{n}_0$) is in the vertical direction since such circular accelerators are dominated by the dipole field which in the absence of strong perturbing fields like spin rotators or snakes set the unperturbed spin precessing axis in the vertical direction. The dominant term in Eq. (1) is

$$\int y'' e^{i\kappa_0\theta(s)}ds = \sum_n kl_n y. \quad (2)$$

Here, we have expanded the integral into a sum of the contributions from each element in the lattice indexed by n, using the thin-lens approximation. Thus, the subscript n denotes the values at each nth element. Considering vertical betatron motion y_β, we obtain,

$$\sum_n kl_n y_\beta = \sum_n kl_n\sqrt{\beta_n}\cos(\mu_n+\phi)e^{i\kappa_0\theta_n}. \quad (3)$$

Here β_n is the vertical betatron function, μ_n the betatron phase and kl_n the integrated quadrupole normalized gradient, and ϕ the initial betatron oscillation phase. A sufficient condition for the cancelation of the intrinsic resonance is if,

$$0 = \sum_m kl_m\sqrt{\beta_m}\cos(\mu_m)$$
$$0 = \sum_m kl_m\sqrt{\beta_m}\sin(\mu_m). \quad (4)$$

Here the sum indexed by m is only over a single string of magnets between two dipoles. The spin precessing terms only change in the dipole, so between dipoles, they are common and can be factored out. Looking first at the FODO cell example,

$$\text{QF O QD O}. \quad (5)$$

Here QF and QD are focusing and defocusing quads, respectively, and O is a drift. In this case, Eq. (2) would become,

$$0 = kl_f\sqrt{\beta_f}\cos(\mu_f) + kl_d\sqrt{\beta_d}\cos(\mu_d)$$
$$0 = kl_f\sqrt{\beta_f}\sin(\mu_f) + kl_d\sqrt{\beta_d}\sin(\mu_d). \quad (6)$$

Since we may always set $\mu_f = 0$, it means that the second equation of Eq. (6) would contain only one term, namely, $kl_d\sqrt{\beta_d}\sin(\mu_d)$. For this term to be zero, either kl_d or β_d would have to be zero or $\sin(\mu_d)$ which implies that $\mu_d = \pi$. In other words, the phase advance across the whole cell would be 2π. So our cell will have no defocusing quad, zero β function at the quad, or an infinitely large β function in the cell.

Thus, using only two quads per cell would not allow us to construct a viable intrinsic spin resonance canceling cell. Introducing a third quadrupole between the dipoles yields,

$$M = \text{QF}_1\text{ O QD O QF}_2\text{ O}. \quad (7)$$

In this case, Eq. (4) would become,

$$0 = kl_1\sqrt{\beta_1}\cos(\mu_1) + kl_2\sqrt{\beta_2}\cos(\mu_2) + kl_3\sqrt{\beta_3}\cos(\mu_3)$$
$$0 = kl_1\sqrt{\beta_1}\sin(\mu_1) + kl_2\sqrt{\beta_2}\sin(\mu_2) + kl_3\sqrt{\beta_3}\sin(\mu_3). \quad (8)$$

In the case that betatron coupling is present another two equations can be added to Eq. (8) which now use μ and β

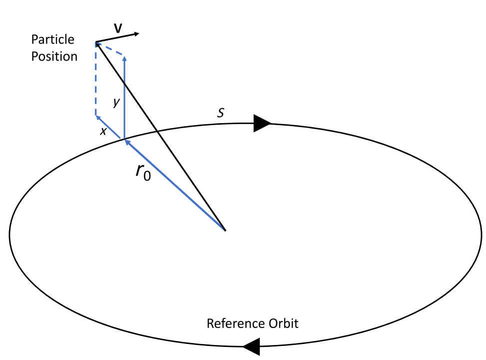

FIG. 1. The curvilinear coordinate system for particle motion in a circular accelerator. The unit vectors $\hat{x}$, $\hat{s}$, and $\hat{y}$ are the transverse radial, longitudinal, and transverse vertical basis vectors; and $\vec{r}_0(s)$ is the reference orbit.

from the horizontal plane. However, in practice, it is probably better to minimize or cancel the coupling source since normally the strength of the horizontal spin resonance due to coupling is much weaker than the normal intrinsic spin resonances.

A. Imperfection spin resonances

Considering the case of vertical motion due to close orbit errors y_{co}, it can be shown that it can be expressed as a sum of the Fourier amplitude of the error harmonic,

$$y_{co} = \sqrt{\beta}\sum_{k=-\infty}^{\infty}\frac{\nu_y^2 f_k e^{ik\mu(s)/\nu_y}}{\nu_y^2 - k^2}$$
$$f_k = \frac{1}{2\pi\nu_y}\oint\sqrt{\beta}\frac{\Delta B_x}{B\rho}e^{-ik\mu(s)/\nu_y}ds \qquad (9)$$

this yields,

$$\sum_n kl_n y_{co} = \sum_{k=-\infty}^{\infty}\frac{\nu_y^2 f_k}{\nu_y^2 - k^2}\sum_n kl_n\sqrt{\beta_n}e^{\frac{ik\mu_n}{\nu_y}}e^{iK\theta_n}. \qquad (10)$$

An equation analogous to Eq. (8) can be developed,

$$0 = kl_1\sqrt{\beta_1}\cos\left(\frac{k\mu_1}{\nu_y}\right) + kl_2\sqrt{\beta_2}\cos\left(\frac{k\mu_2}{\nu_y}\right) + kl_3\sqrt{\beta_3}\cos\left(\frac{k\mu_3}{\nu_y}\right)$$
$$0 = kl_1\sqrt{\beta_1}\sin\left(\frac{k\mu_1}{\nu_y}\right) + kl_2\sqrt{\beta_2}\sin\left(\frac{k\mu_2}{\nu_y}\right) + kl_3\sqrt{\beta_3}\sin\left(\frac{k\mu_3}{\nu_y}\right). \qquad (11)$$

Since the strength of the imperfection spin resonance is dominated by values when $k \approx \nu_y$, we find that imperfection spin resonances are typically minimized when Eq. (8) is satisfied. Thus, minimizing intrinsic resonances will help minimize the net imperfection resonances. Using the accelerator modeling code MADX [9] and one of its native optimizers, one can find the quadrupole strengths that satisfy Eq. (8) and yield a stable lattice. In the following section, we explore several lattices to see how applying these spin canceling type of cells might be applied to improve polarization transmission for both proton and electron machines.

IV. ACCELERATOR EXAMPLES

We explore a few types of accelerators and how they might benefit from using these design approaches. We first consider the AGS's booster then the AGS machine. Next, we look at toy lattices on the scale of the proposed Future Circular Collider (FCC) for both electrons and hadrons. This is also very similar in scale to the proposed CEPC accelerator.

TABLE I. BNL's AGS booster design.

Bending radius (m)	13.75
Circumference (m)	201.78
Q_x	4.62
Q_y	4.6
Cell length (m)	8.4075
Quad length (m)	0.50375
K1	0.548
K2	−0.550
β_x MAX (m)	13.3
β_y MAX (m)	13.5
D_x MAX (m)	3.95
No. of FODO cells	24
Peak dipole field (T)	1.27
Peak possible $a\gamma$	10[a]
Injection energy (MeV)	200
Typical extraction (GeV)	1.5

[a]Based on peak dipole field.

A. BNL's AGS booster example

The key parameters for BNL's AGS booster are shown in Table I. The booster has 36 2.4 m long dipoles with a bending radius of 13.75 m. Each arc FODO cell is 8.4075 m, and quadrupoles are 0.50375 m long. The total circumference is 201.78 m with six superperiods made up of four FODO cells per period, two of which are missing a dipole.

In our test case, we inserted three quadrupoles families into each half cell and increased the arc cell length from 8.4075 to 9.5 m to accommodate the new quadrupoles, yielding a circumference of 228 m. In this case, we first minimized Eq. (8) for each cell type using the MADX Simplex optimizer over a total of 12 families of quadrupoles (3 for each of the 4 cells). We did this while controlling the maximum β functions and dispersion. Next, we used the DEPOL algorithm in Python to minimize the spin resonance contribution for each cell again controlling the maximum β functions and dispersion. The results of the quadrupole strengths and Twiss parameters for each case are listed in Table II and the spin resonances to $a\gamma < 10$ are plotted in Fig. 2. In all cases, we use a standard normalized emittance of 10 mm mrad for the calculation of the intrinsic spin resonances. Optics for the thin-lens optimized lattice are shown in Fig. 4. The MADX optimization using the thin-lens approximation brought Eq. (8) to less than 10^{-8} and significantly reduced the resonance strength, yet we are still left with residual resonance amplitude. Optimization using the full spin resonance integral as calculated in DEPOL improved upon this as shown in Fig. 3.

In addition to lengthening the arc cells by about 1 m, an additional four quadrupoles would need to be added per arc

TABLE II. Modified AGS booster lattice.

	Thin lens	DEPOL
Bending radius (m)	13.75	
Peak dipole field (T)	1.27	
Peak possible $a\gamma$	10	
Circumference (m)	228	
Cell length (m)	8.4075	
Quad length (m)	0.50375	
No. of quads	144	
Q_x	4.62	4.9835
Q_y	1.82	0.739
C_x	−9.98	−10.5
C_y	−15.08	−31.35
β_x MAX (m)	26.11	60.42
β_y MAX (m)	12.16	12.31
D_x MAX (m)	6	5.6
Peak quad field (T/m)	17	16.9

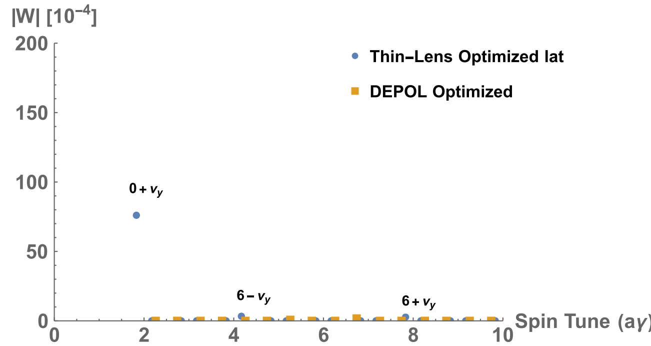

FIG. 3. DEPOL calculated spin resonances using normalized emittance of 10 mm mmrad. Here we use the special intrinsic spin resonance suppressing cell for the booster. Here the thin-lens optimized optics using Eq. (8) and optics optimization using the DEPOL algorithm are compared. The strongest intrinsic spin resonances are labeled.

cell or 96 with a maximum peak field of about 15 T/m, while this is technically feasible, it is costly. Another approach would be to build a 16 superperiodic lattice around the 36 dipoles and 48 quadrupoles. For this lattice, if we kept the vertical tune below the a factor of 1.7928, it would place all the spin resonances outside the energy range of the booster. This is because there would be no $0 + \nu$ spin resonance since the spin tune could never be lower than a. The next spin resonance would occur no lower than $a\gamma = 16 - a = 14.2072$. This would not require satisfying Eq. (8) and one could use traditional FODO cells. To achieve this, only hinges on boosting the periodicity to 16, keeping the tune below a and maintaining enough drift space for the rf systems, sextupoles, and correctors.

B. AGS-sized machine

The AGS lattice parameters are listed in Table III: It is made up of 12 superperiods each containing 20 combined function magnets of long and short lengths. The use of combined function magnets makes the use of Eq. (8) problematic since it mixes up the dipole spin precession with the quadrupole spin kicks. However, one could propose a new lattice using separate dipoles and quadrupoles of the same periodicity and approximately the same circumference. In this case, one could choose a higher periodicity and either a high or low vertical tune to completely avoid all the spin resonances in the energy range from 0 to 48.

However, for the sake of demonstrating the utility of spin resonance canceling cells, we consider the low 12 periodicity building a lattice using Eq. (8) which kept the spin resonance strengths much lower than in the current AGS.

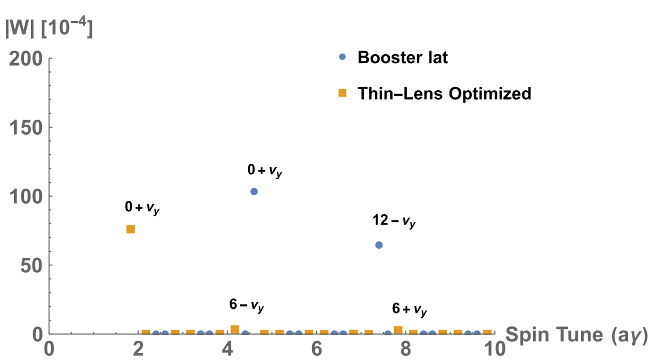

FIG. 2. DEPOL calculated spin resonances using vertical emittance of 10 mm mrad with the lattice employing the special intrinsic spin resonance suppressing cell. This is compared to a standard FODO cell with dipoles in-between BNL's booster lattice. Here the strongest intrinsic spin resonances are labeled.

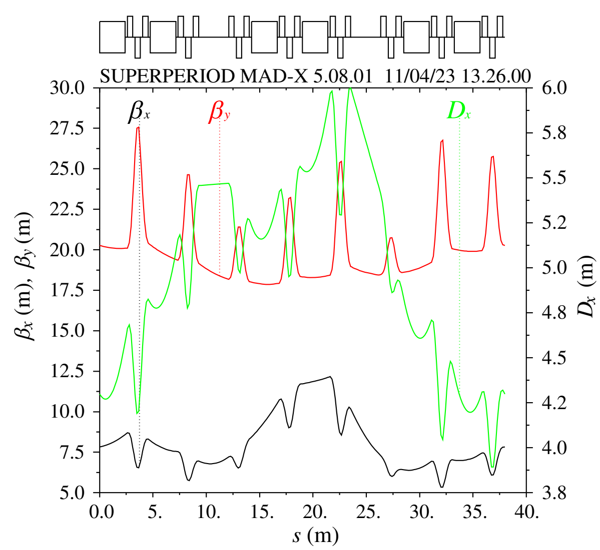

FIG. 4. β functions for horizontal and vertical planes and dispersion in the horizontal plane are shown for one superperiod of the new booster lattice. In this case, it is optimized using Eq. (8).

TABLE III. BNL's AGS lattice.

Bending radius (m)	85.3785
Circumference (m)	807.09
Q_x	8.847
Q_y	8.88
β_x MAX (m)	34.05
β_y MAX (m)	50.8
D_x MAX (m)	5.64
Peak possible $a\gamma$	36[a]
Typical injection energy (GeV)	1.5
Typical extraction energy (GeV)	25

[a]Based on peak dipole field.

TABLE IV. Three quad AGS-like lattice.

Bending radius (m)	85.3785
Peak dipole field (T)	1.0
Peak possible $a\gamma$	10
Circumference (m)	811.2
Cell length (m)	16.15
Quad length (m)	0.6
No. of quads	144
Q_x	11.23
Q_y	3.24
C_x	−27
C_y	−45
β_x MAX (m)	58.95
β_y MAX (m)	19.3
D_x MAX (m)	5.86
Peak quad field (T/m)	46.75

Here, we use a lattice with 12 superperiods made up of 4 dipoles with 3 quadrupoles between the dipoles and a 3 m straight connecting the super-periods. The key parameters of this lattice are listed in Table IV and the optics are plotted in Fig. 5.

In Fig 6, we show a comparison of DEPOL calculated intrinsic spin resonances for the standard AGS lattice and the toy AGS-like lattice.

C. Electron machines below 20 GeV

Normally, for high energy electrons, the vertical emittance damps toward zero and the effect of vertical intrinsic spin resonances can be negligible. The effects of imperfection spin resonances tend to dominate. However, for electrons at energies where the damping time is much longer than its acceleration time, crossing strong vertical intrinsic spin resonances has the potential to lead to strong depolarization effects as in the case of EIC's proposed electron injector. One could also consider an optimized AGS-sized electron machine, using a lattice like we just developed for the protons. Such a machine would be limited to 15 GeV since above this radiated power per turn would be considerable and go above 50 MeV per turn.

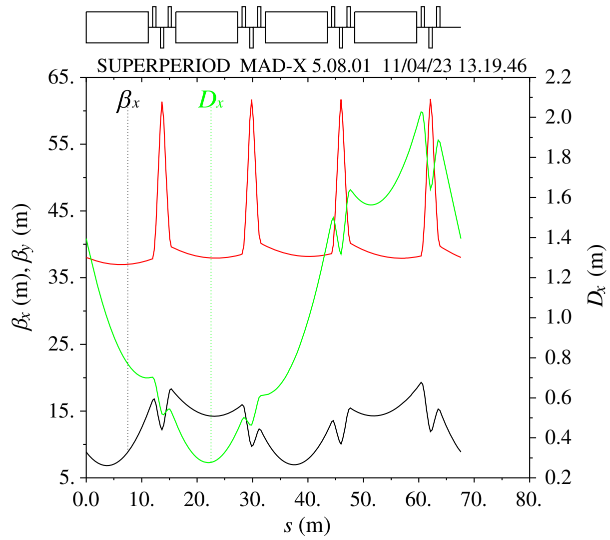

FIG. 5. β functions for horizontal and vertical planes and dispersion in the horizontal plane are shown for one superperiod of the new AGS lattice. In this case, it is optimized using Eq. (8).

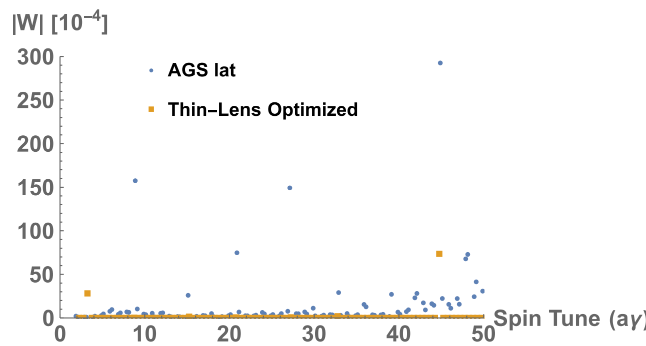

FIG. 6. DEPOL calculated spin resonances for the proton AGS machine and the toy AGS-like machine with periodicity of 12 and spin cell suppression.

An additional benefit of such a lattice is that not only will the intrinsics be avoided or minimized but the imperfections will also be minimized.

D. FCC-like machines

The proposed FCC-ee and Circular Electron Positron Collider (CEPC) are both positron and electron colliders with a circumference of around 100 km reaching top collision energies of above 100 GeV. Considering the energy for the FCC-ee booster with injection energy at 20 GeV and top extraction energy of 182.5 GeV in terms of $a\gamma$, ranges from 45 to 414. Choosing a periodicity of 500 if the arc tunes are kept above 45 units and the construction circular with a straight section confined to the 200-m long arc cell then all spin resonances can be avoided. If longer symmetry breaking straight sections are needed, then an approach used for the EIC's RCS to suppress and cancel the

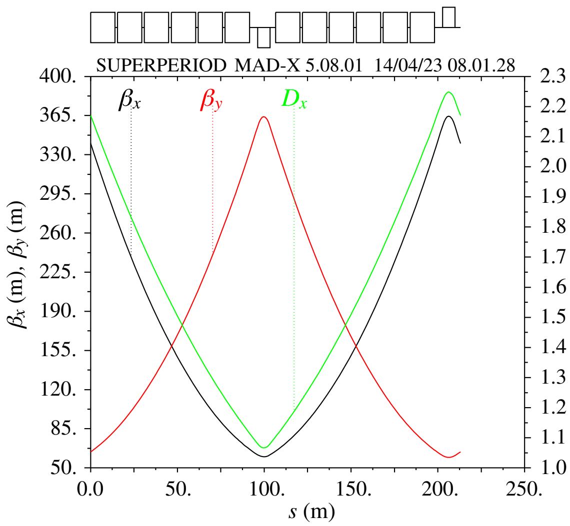

FIG. 7. β functions for horizontal and vertical planes and dispersion in the horizontal plane are shown for one FODO cell of the arc FCC-h lattice (per 2019 CDR).

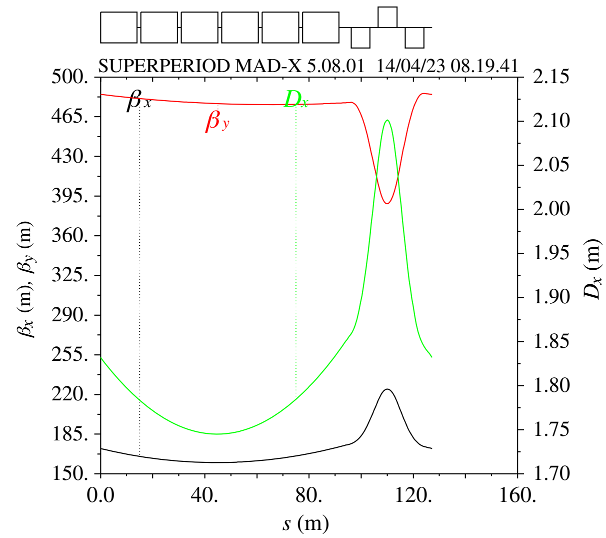

FIG. 8. β functions for horizontal and vertical planes and dispersion in the horizontal plane are shown for one dipole to dipole (similar to half standard FODO cell) of my Toy arc only FCC-h lattice.

resonance contribution from these sections can be used. This would be easier to accomplish if sufficient room in the tunnel is made so that the booster would not need to bend around the experimental halls. In the case of the CEPC booster, studies are ongoing which exploit high periodicity to minimize polarization losses [10]. In their case symmetry breaking due to insertions limit this approach, but it might be possible to employ the spin canceling approaches developed in this paper for their insertion sections.

The FCC-hh is also proposed which will accelerate protons to energies from 3 TeV using the LHC as a booster to 50 TeV. The rough optics are shown in Fig. 7 for the arc FODO cell and in Table V, the parameters for a simplified arc only model (no insertion sections) is shown. This simplified model only has dipoles and quadrupoles using the same bending radius, magnet lengths of the dipoles, and quadrupoles as defined in “FCC-hh: The Hadron Collider Future Circular Collider Conceptual Design Report Volume 3” [11].

The energy ranges from 3 to 50 TeV in $a\gamma$ space is 5732 to 95 532. In this case, a periodicity high enough to avoid spin resonances is not reasonable. However, the arc cells could be constructed with three quadrupoles between the dipoles to achieve a major suppression of the spin resonances. In this case, using 1 focusing and 2 defocusing quadrupoles placed in a 1/2 arc cell of 127.23-m long with a 42.58° phase advance in the horizontal and 15.48° in the vertical plane kept all intrinsic resonances in the energy range less than 1 at 10 mm mrad normalized emittance.

TABLE V. FCC-h arc only standard lattice.

Bending radius (km)	10.427
Peak dipole field (T)	16
Peak possible $a\gamma$	95532
Circumference (arc only) (km)	83.081
Cell length (m)	213.03
Periodicity	390
Q_x	99.83
Q_y	100.57
C_x	−129.22
C_y	−130.03
β_x MAX (m)	355.5
β_y MAX (m)	354.99
D_x MAX (m)	2.22
Arc packing factor	0.78
Peak quadrupole gradient (T/m)	320[a]

[a]CDR has 367 T/m

TABLE VI. FCC-h arc only three quad optimized lattice.

Bending radius (km)	10.427
Peak dipole field (T)	16
Peak Possible $a\gamma$	95532
Circumference (arc only) (km)	99.239
Cell length (m)	254.46
Periodicity	780
Q_x	92.35
Q_y	33.71
C_x	−80.59
C_y	−74.91
β_x MAX (m)	214.79
β_y MAX (m)	485.60
D_x MAX (m)	2.05
Packing factor	0.66
Peak quadrupole gradient (T/m)	610[a]

[a]Scaled value based on CDR peak quadrupole value would be 699 T/m

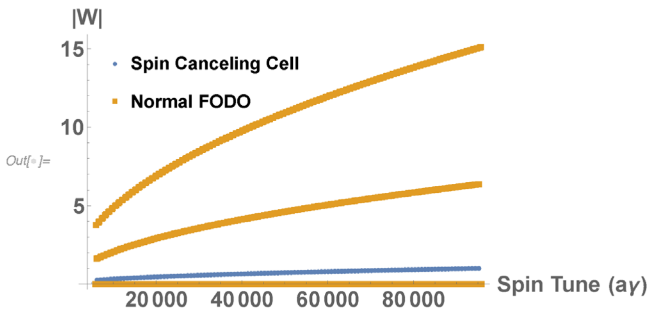

FIG. 9. DEPOL calculated spin resonances for a FCC-hh arc only (no insertions) lattice using standard FODO cell construction versus an FCC-hh like lattice with three quad arc cells which suppress the spin resonances.

This is low enough that six snakes should be sufficient to control the intrinsic spin resonances. The optics for one arc half cell are plotted in Fig. 8 and the parameters are listed in Table VI. In this case, the periodicity is 2 times higher since our repeating period is from dipole to dipole and the insertion of two more quads increased the path length due to the arc to 99 km. This compares to an FCC-hh lattice which following a standard FODO lattice design using an arc cell of 213 m with an arc path length of 83 km, would give resonances greater than 15 at 10 mm mrad normalized emittance. In Fig. 9, we can see a comparison between the two FCC-hh lattice's intrinsic spin resonance strength. The three quadrupole lattice would also require effectively doubling the peak strength for the quadrupole which might require increasing the length of the quadrupole if the peak fields could not be raised. Additionally, this construction would reduce the packing factor from 0.78 to 0.66.

V. CONCLUSION AND FURTHER STUDY

Using intrinsic resonance canceling arc cells, one can build up a whole ring with all sorts of broken symmetry and still avoid or greatly reduce strong intrinsic depolarizing spin resonances. However, one of the challenges is to build these cells in such a way that the β functions and dispersion are controlled. As well their natural dynamic aperture and chromatic features should be studied to better understand the optimal configuration.

ACKNOWLEDGMENTS

Work supported by U.S. DOE under Contract No. DE-SC0012704 with the U.S. Department of Energy.

[1] Y. S. Derbenev and A. M. Kondratenko, Dokl. Akad. Nauk Ser. Fiz. **223**, 830 (1975), https://inspirehep.net/literature/103800.

[2] I. Koop, in *Proceedings of 55th ICFA Advanced Beam Dynamics Workshop on High Luminosity Circular e+e- Colliders—Higgs Factory* (2015), p. SAT3A3, https://inspirehep.net/files/62801cefe65380f62c0535b6a810d3cc.

[3] V. H. Ranjbar *et al.*, Phys. Rev. ST Accel. Beams **7**, 051001 (2004).

[4] A. Lehrach, R. Gebel, R. Maier, D. Prasuhn, and H. Stockhorst, Nucl. Instrum. Methods Phys. Res., Sect. A **439**, 26 (2000).

[5] K. Steffen, On spin dispersion, harmonic spin matching and orbit tuning, DESY, Technical Report No. DESY-HERA-82-02, 1982, https://lib-extopc.kek.jp/preprints/PDF/1982/8206/8206129.pdf.

[6] A. W. Chao and Y. S. Derbenev, Part. Accel. **36**, 25 (1991), https://cds.cern.ch/record/1108247/files/p25.pdf.

[7] V. H. Ranjbar, M. Blaskiewicz, F. Méot, C. Montag, S. Tepikian, S. Brooks, H. Witte, I. Marneris, V. Ptitsyn, and F. J. Willeke, Phys. Rev. Accel. Beams **21**, 111003 (2018).

[8] E. D. Courant and R. D. Ruth, The acceleration of polarized protons in circular accelerators, Brookhaven National Laboratory, Upton, NY, Technical Report No. BNL-51270, 1980.

[9] CERN—BE/ABP Accelerator Beam Physics Group, Methodical accelerator design: Mad-x v5.07, https://madx.web.cern.ch/madx/.

[10] Z. Duan, T. Chen, J. Gao, D. Ji, X. Li, D. Wang, J. Wang, Y. Wang, and W. Xia, in Proceedings of 65th ICFA Advanced Beam Dynamics Workshop on High Luminosity Circular e^+e^- Colliders, Frascati, Italy (JACoW, Geneva, Switzerland, 2023).

[11] A. Abada *et al.* (FCC Collaboration), Eur. Phys. J. Spec. Top. **228**, 755 (2019).